



# *F*ox: Focus Anywhere for Fine-grained Multi-page Document Understanding

Chenglong Liu<sup>1</sup>\*, Haoran Wei<sup>2</sup>, Jinyue Chen<sup>1</sup>, Lingyu Kong<sup>1</sup>, Zheng Ge<sup>2</sup>,  
Zining Zhu<sup>1</sup>, Liang Zhao<sup>2</sup>, Jianjian Sun<sup>2</sup>, Chunrui Han<sup>2</sup>, Xiangyu Zhang<sup>2</sup>

<sup>1</sup>University of Chinese Academy of Sciences, <sup>2</sup>MEGVII Technology  
<https://ucaslcl.github.io/foxhome/>

## Abstract

Modern LVLMs still struggle to achieve fine-grained document understanding, such as OCR/translation/caption for regions of interest to the user, tasks that require the context of the entire page, or even multiple pages. Accordingly, this paper proposes **Fox**, an effective pipeline, hybrid data, and tuning strategy, that catalyzes LVLMs to focus anywhere on single/multi-page documents. We introduce a novel task to boost the document understanding by making LVLMs focus attention on the document-level region, such as redefining full-page OCR as foreground focus. We employ multiple vision vocabularies to extract visual hybrid knowledge for interleaved document pages (*e.g.*, a page containing a photo). Meanwhile, we render cross-vocabulary vision data as the catalyzer to achieve a full reaction of multiple visual vocabularies and in-document figure understanding. Further, without modifying the weights of multiple vision vocabularies, the above catalyzed fine-grained understanding capabilities can be efficiently tuned to multi-page documents, enabling the model to focus anywhere in both format-free and page-free manners. Besides, we build a benchmark including 9 fine-grained sub-tasks (*e.g.*, region-level OCR/summary, color-guided OCR) to promote document analysis in the community. The experimental results verify the superiority of our model.

## 1 Introduction

Recently, research on Large Vision-Language Models [1, 25, 48] has been an attractive direction. These models not only easily handle some conventional vision tasks (*e.g.*, Image Caption [37], OCR [22]), but also demonstrate powerful reasoning capabilities like humans.

The LVLMs mostly give responses by leveraging large language models [8, 30, 45] to follow language instructions while referring to the vision vocabulary to understand the input image. Some researchers attempt to adopt LVLMs to advance the understanding of large-resolution (*e.g.*,  $833 \times 1132$ ) document pages. For example, UReader [42] crops the input image into smaller patches to align with a CLIP-style vision vocabulary of input size  $224 \times 224$ . Later, TextMonkey [18] divides the input image into  $448 \times 448$  patches and uses Openclip’s ViT-bigG [13] along with a resampling strategy to retain useful image tokens. LLaVA-NeXT [16] adopts CLIP-ViT-L-336px to perform visual perception and splits the input image into smaller patches to encode independently. InternVL-V1.5 [7] proposes a stronger vision vocabulary InternViT-6B with the input size of  $448 \times 448$ . Similarly, to capture more details of the input image, InternVL-V1.5 [7] dynamically divides the input image into 1 to 12 tiles. Different from the methods above, without cropping patches, Vary [38] writes an extra SAM-style [14] vision vocabulary specific to document and chart data, running in parallel with the CLIP branch. Vary can directly encode  $1024 \times 1024$  page into 256 image tokens with a high compression ratio.

\*This work was done when the first author was interning at Megvii Technology Inc.

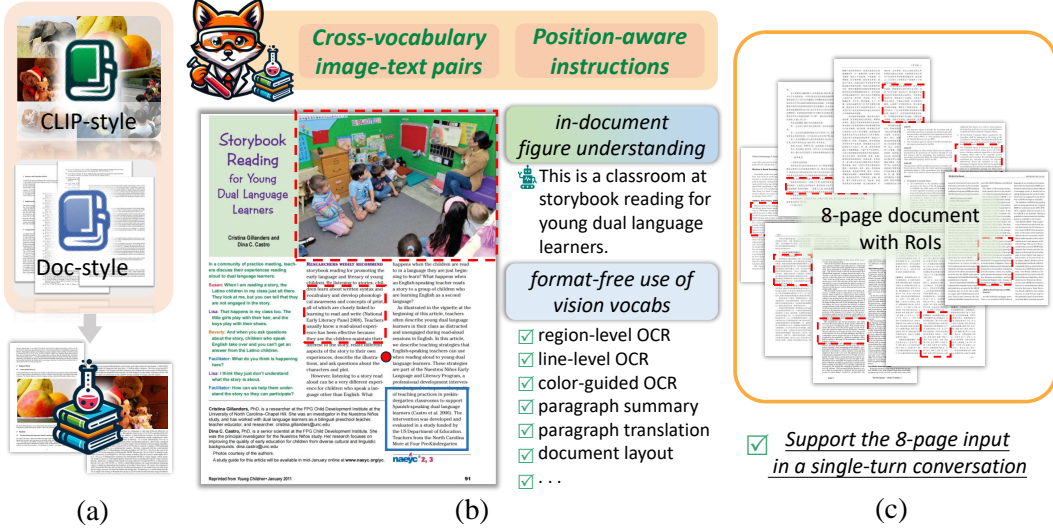


Figure 1: (a) Multiple vision vocabularies are catalyzed using synthetic cross-vocabulary data to handle interleaved pages. (b) Fox achieves fine-grained document-level understanding by focusing anywhere, such as region-level OCR/translation and in-page figure caption. (c) Fox impressively supports the entire 8-page input and can focus on multiple cross-page RoIs in a single-turn conversation.

The patch-based models [7, 16, 18, 42] mostly employ CLIP-style vision vocabulary with small resolution, so a large-scale document needs to be decomposed into many patches/tiles. A patch/tile is independently encoded to 256 image tokens, and InternVL-V1.5 [7] even produces 3,328 image tokens during training. However, numerous image tokens are difficult to extend to multi-page documents for contextual understanding. More importantly, there may still be dense characters on these cropped patches, but CLIP-style vision vocabulary compresses limited sparse information of small input images via global contrastive learning, preventing these models from losslessly recovering the content of the original document (e.g., full-page OCR). Although Vary [38] enjoys a high compression ratio and avoids cropping patches by directly encoding the document page, the lack of full collaboration across multiple vision vocabularies limits the performance. For example, given an input document page, Vary [38] tends to only activate the SAM-style ViT branch due to the specific-vocabulary visual bias. In addition, the above models are sensitive to document format (e.g., multi-column) and do not support fine-grained user interaction on specific regions on documents.

Another key point for the document understanding is how to carry out fine-grained interaction, such as OCR/summarizing/captioning a region of interest. Actually, LVLMS with human-like referential dialogue capability for natural scenes have been investigated, such as Shikra [6] and ChatSpot [46]. They introduce referring spatial coordinates to refer to the special region of the input natural image, lifting the user experience and leading to more precise conversations. But these models can not handle the document images due to vision vocabulary CLIP-ViT [28] which is specific to natural scenes and has low input resolution. Besides, CLIP-style pre-training method based on Laion-COCO [31] (image-phrase pairs) only weakly write sparse visual knowledge, leading to a gap in understanding the dense document. Thus, we may ask: *Can we devise an effective and efficient pipeline for LVLMS to achieve the fine-grained multi-page document understanding?*

In this paper, we propose Fox, an effective pipeline, hybrid data, and tuning strategy, giving a pleasing answer to the above question. The proposed Fox efficiently catalyzes the LVLMS's attention to anywhere on single/multi-page documents in a user-friendly manner. Our solution has three highlights: 1) *Focusing anywhere*: We introduce a novel task that boosts document understanding by focusing on the region of interest via fine-grained position-aware prompts, *i.e.*, click points, dragged bounding boxes, and drawn color boxes. Notably, the dense full-page OCR sub-task can be further optimized by being redefined as foreground focus. 2) *Full reaction across multiple vision vocabularies*: To fully interpret hybrid visual knowledge on interleaved document pages, we synthesize cross-vocabulary vision data to activate multiple visual vocabularies simultaneously to break down the specific-vocabulary bias of visual content, catalyzing multiple vision vocabularies

to a full reaction. 3) *Supporting multi-column format and multiple pages*: With the position-aware prompts, the pipeline of focusing anywhere can yield robust performance regardless of document format. Moreover, benefiting from the high compression ratio (one  $1024 \times 1024$  page to 256 image tokens), we demonstrate the Fox can be efficiently tuned to achieve the above fine-grained capabilities on multi-page documents without modifying parameters of vision vocabulary.

As a result of the focusing catalytic process, the proposed Fox can not only give specific-vocabulary responses (*e.g.*, page foreground OCR, region/line-level OCR/translation) but also gain the noticeable ability to utilize the cross-vocabulary visual knowledge (*e.g.*, color-guided OCR, in-document figure caption). Furthermore, for more impressive multi-page document features, Fox can give the OCR results of  $region_1$  on  $page_1$  and  $region_n$  on  $page_n$  by only one question. Note that tasks like this with reference to cross-page content are of great research significance. We encourage researchers to rethink the framework design for LVLm-based document understanding and not be limited to conventional single-page sparse QA tasks. Our contributions can be summarized as follows:

- We introduce a series of novel tasks to boost document understanding by enabling LVLms to focus on document-level regions of interest. We propose an effective and efficient solution named Fox to focus anywhere on single/multi-page documents.
- To catalyze multiple vision vocabularies for figure-text interleaved documents, we provide methods for generating hybrid data containing cross-vocabulary visual elements.
- Fox is robust to documents of various formats due to the flexible position-aware prompts. Without training vision vocabulary, our Fox can be easily tuned to multi-page documents and gain cross-page parsing capabilities.
- We build a fine-grained document benchmark, including 9 sub-tasks, such as dense page OCR, region-level OCR/translation/summary, color-guided OCR, multi-page OCR/VQA. Experimental results show that our Fox outperforms other LVLms by a large margin.

## 2 Related Works

### 2.1 Visual Document Understanding

Visual document understanding is widely investigated in the research field of computer vision. Optical Character Recognition (OCR) is a basic task, which plays a key role in document digitalization [23, 32]. The layout analysis task [47] aims to detect various document elements and facilitate to understanding of spatial relationships between them. We believe that OCR is a good task to test whether LVLms can compress documents losslessly. Besides, for translation and summary [11, 36] tasks, the proposed Fox can directly give answers for document images via the multimodal framework.

### 2.2 Large Language Models

In recent times, the success of LLMs has ignited the fields of natural language processing (NLP) and artificial general intelligence (AGI). The LLMs are built with the popular transformer framework which is explored by earlier NLP research, *e.g.*, BERT [10], GPT-2 [29], T5 [30], and so on. Afterward, it is discovered that when the model parameters are expanded to a certain size, the language model will be greatly boosted due to the so-called "emergent ability" [40]. Further, the "GPT time" comes with amazing dialogue robots optimized by Reinforcement Learning with Human Feedback [9], *e.g.*, InstructGPT [26] and ChatGPT [24]. Following that, OPT [45], LLaMA [35], and GLM [44] are accessible to the community to pursue the performance like the GPT family. Based on the open-source LLMs, for more specific requirements, some fine-tuned models have merged, such as Alphaca [33] and Vicuna [8], which also play critical roles in later Large Vision-Language Models.

### 2.3 Large Vision-Language Models

For vision-centric tasks, Large Vision-Language Models (LVLms) [1, 17, 21] have been developed by connecting the vision networks to LLMs. CLIP-ViT [28] is a mature pre-trained vision vocabulary widely used to inject visual modality into language models. To ensure that LLMs can understand the visual context, LLaVA [17] places the linear layers to project visual tokens into text space. Later, beyond natural scenes, LVLms for large-resolution documents have emerged. UReader [42] is

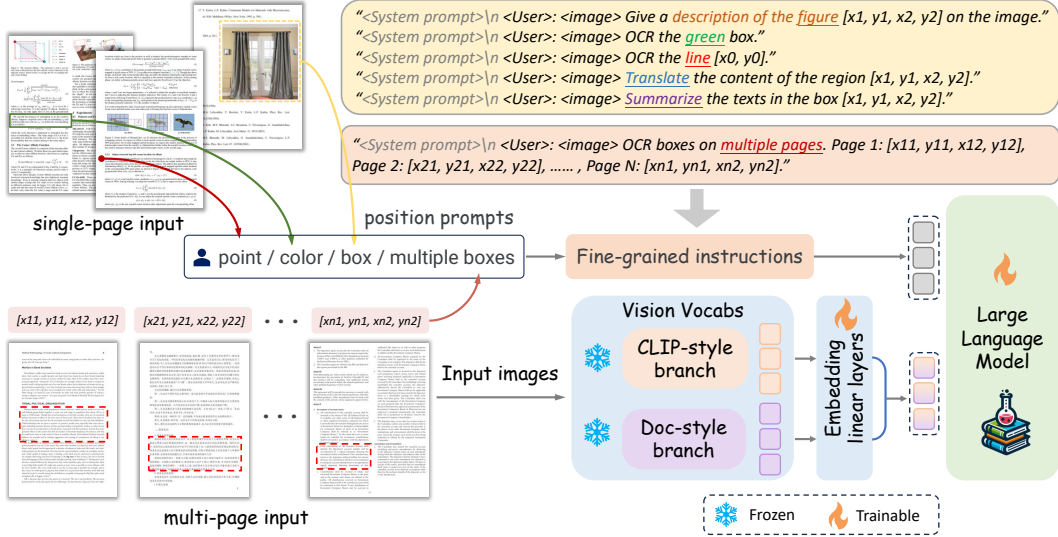


Figure 2: Overall framework of the proposed Fox. All image tokens of multiple pages are unified into a sequence to achieve multi-page understanding. We devise position-aware prompts (point, color, and box) to make the model focus anywhere on single/multi-page documents. We catalyze multiple vision vocabularies into a full reaction of hybrid visual knowledge for interleaved pages.

developed based on the LVLM mPLUG-Owl [43]. UReader [42] devise a shape-adaptive approach to crop input images into  $224 \times 224$  patches and feed them into CLIP vision encoder. Following Qwen-VL [3], TextMonkey [18] uses a more powerful vision vocabulary Openclip’s ViT-bigG [13] with  $448 \times 448$  input size to endoce each cropped patch. With the strategy of cropping patches, LLaVA-NeXT [16] adopts CLIP-ViT-L-336px to perform visual perception. Similarly, to capture more details, InternVL-V1.5 [7] dynamically divides the input image into 1 to 12 tiles of  $448 \times 448$ . In contrast, without cropping patches, Vary [38] writes an extra SAM-style [14]  $1024 \times 1024$  vision vocabulary specific to document and chart data, running in parallel with the CLIP branch.

Compared to the above models, we believe that document understanding should move towards more fine-grained (*e.g.*, region-level OCR/translation) and multi-page tasks. Imagine how cool it would be if we could use the LVLM like a reading pen! In this paper, we introduce Fox which can achieve fine-grained features by focusing anywhere on multi-page documents.

### 3 Methods

In this section, we will elaborate on the details of the proposed Fox. First, we introduce the flexible pipeline which supports single/multi-page document understanding. Second, we provide the strategy to produce the data containing hybrid visual elements to activate multiple vocabularies concurrently. Last, we unify multi-task data with position-aware prompts to conduct the focusing process.

#### 3.1 Framework for Focusing Anywhere

As illustrated in Figure 2, the architecture of the proposed Fox is built with two vision vocabularies, a large language model, and embedding linear layers. Specifically, to better handle figure-text interleaved large-resolution documents, there are two vision vocabularies, including natural content-aware CLIP-ViT [28] and artificial content-aware Vary-tiny [38]. The overall framework is neat and provides more user-friendly fine-grained interactions, which can focus on the entire page and more specific regions of interest (RoI). Impressively, the proposed Fox also supports users to select RoIs on multiple pages at the same time, enabling cross-page contextual understanding.

Given a set of input document pages  $I = \{p_i\}_{i=1}^N$ , users can further indicate regions of interest  $r_i$  on each page by clicking a point, dragging boxes, or drawing color boxes, and then give some language instructions  $L^{instruct}$  about the questioning RoIs.  $N$  is the number of input pages. The

spatial coordinates or color information of  $\{r_i\}_{i=1}^N$  is transformed into position-aware prompts and combined with  $L^{instruct}$  to produce complete referential instructions. Meanwhile, two vision vocabularies will produce 256 image tokens  $v_i^C \in \mathbb{R}^{256 \times 1024}$  and  $v_i^S \in \mathbb{R}^{256 \times 1024}$  for each page  $p_i$ . These image tokens  $\{v_i^C\}_{i=1}^N$  and  $\{v_i^S\}_{i=1}^N$  are sent into linear layers  $W^C$  and  $W^S$  to align with linguistic space. Then, the final image tokens  $v_i \in \mathbb{R}^{256 \times 2048}$  can be obtained by concatenation. Note that  $v_i$  is compressed into cross-vocabulary content, including dense characters and figures. Finally, with the projected image tokens and referential instructions, LLM will generate the response sequence  $Q$  in an auto-regressive manner. The above process can be formulated as follows:

$$\{v_i\}_{i=1}^N = [W^C \circ \{v_i^C\}_{i=1}^N || W^S \circ \{v_i^S\}_{i=1}^N] \quad (1)$$

$$Q = \mathcal{L} \mathcal{L} \mathcal{M} (\{v_i\}_{i=1}^N, (L^{instruct}, \Psi(\{r_i\}_{i=1}^N))) \quad (2)$$

where  $[||\cdot]$  is the concatenation operation.  $\Psi(\cdot)$  denotes the normalization for spatial coordinates. Note that multi-page ( $N$  pages) image tokens  $\{v_i\}_{i=1}^N$  are unified into a sequence for cross-page contextual understanding. With the causal masked sequence modeling, the training objective can be expressed as:

$$\mathcal{L}_t = -E_{(Q,V) \sim D} \log P_\theta (q_m | q_{< m}, \{v_i\}_{i=1}^N) \quad (3)$$

where  $m$  denotes the current index of the target token and  $D$  is the multi-page multi-grained dataset.

### 3.2 Activating Multiple Vision Vocabularies by Cross-Vocabulary Hybrid Data

We hope to catalyze new capabilities more efficiently while freezing pre-trained multiple vision vocabularies. Note that each vocabulary is written with visual knowledge of its specific-domain data. CLIP [28] using 400M [31] image-text pairs is geared toward perceiving natural images, and Vary-tiny [38] using about 10M artificial data is good at page-level documents. There is a specific-vocabulary perceptual bias during querying vision vocabs due to the simple stacking of samples in two domains. Hence, we synthesize hybrid data containing the cross-vocabulary elements for the full reaction of multiple vision vocabularies. Instead of focusing too much on a specific vocabulary, richer cross-visual knowledge will be activated by breaking down the barriers of visual content.

**Preparing PDF data.** We download enough open-source files in PDF format from e-books, CC-MAIN, and arXiv. Then, we parse the PDFs with some useful Python packages. We save each document page as a PNG-style image. Meanwhile, we locate each potential paragraph/line and record the corresponding bounding box and text content within it.

**Figure-text interleaved data.** We choose the BLIP558k [17], Laion-COCO [31], and Region-Chat [46] datasets that contain descriptions for natural images, and we randomly sample the same number of document pages from the prepared PDF data. Clearly, before we render a natural image of  $W^n \times H^n$  pixels into a document page with the resolution of  $W^d \times H^d$  pixels, we should make the size of the natural image smaller than that of the document page. The scaling process can be formulated as follows:

$$\begin{cases} W_{new}^n = \text{randint} \left( \left[ \alpha \cdot W^d \right], \left[ \beta \cdot W^d \right] \right), H_{new}^n = \lfloor W_{new}^n / W^n \cdot H^n \rfloor, & \text{if } W^n / H^n > W^d / H^d \\ H_{new}^n = \text{randint} \left( \left[ \eta \cdot H^d \right], \left[ \gamma \cdot H^d \right] \right), W_{new}^n = \lfloor H_{new}^n / H^n \cdot W^n \rfloor, & \text{if } W^n / H^n \leq W^d / H^d \end{cases} \quad (4)$$

where  $W_{new}^n / H_{new}^n$  denote the desired width/height of the scaled natural image.  $\lfloor \cdot \rfloor$  means the integral function.  $\alpha, \beta, \eta$ , and  $\gamma$  are the hyperparameters that control the scaling ratio, and they are set to 0.3, 0.9, 0.4, and 0.9, respectively. Then, we randomly pick a suitable location  $(x_1^n, y_1^n, x_2^n, y_2^n)$  on the page to place the scaled natural image. What's more, to make the interleaved data reasonable and delete the occluded text on this page, we calculate the intersection of union (IoU) between  $(x_1^n, y_1^n, x_2^n, y_2^n)$  and the vanilla text boxes  $\{(x_{i,1}^d, y_{i,1}^d, x_{i,2}^d, y_{i,2}^d)\}_{i=1}^{N_d}$ , and fill the text boxes overlapped by the natural image with the white color.  $N_d$  is the number of text boxes on this document page. So, we can obtain cross-vocabulary image-text pairs for in-document figure caption. The text for each interleaved page includes the filtered optical characters and the description of the pasted natural image.

**Color-text hybrid data.** CLIP is written with the knowledge for recognizing colors, while the Vary-tiny is not. We produce color-text hybrid data to further activate multiple vocabularies, which is the key to enabling Fox to support the conversations for users' color-guided RoI. We randomly select three text boxes and paint them directly on the document page in red, blue, and green colors. The proposed Fox is expected to directly give the OCR results in the area with the questioning color.



### 3.3 Triggering Focusing Process via Fine-grained Instruction-following Tasks

We devise fine-grained instructions based on several position-aware text prompts, such as points, boxes, and colors, to catalyze Fox to focus any fine-grained region on single/multi-page documents.

**Fine-grained document understanding.** We define several novel sub-tasks to drive the model to focus on fine-grained regions for flexible document-level understanding: 1) Foreground OCR. We redefine the page OCR task as the foreground focus to further boost the dense perception. The instruction can be “Give the OCR results of the box  $(x_{i,1}^f, y_{i,1}^f, x_{i,2}^f, y_{i,2}^f)$ ”. The foreground box can be obtained by some simple operations. 2) Region-level OCR. Based on the obtained text boxes, we transform the content of one page into multiple region-level OCRs via multi-turn conversations. An example can be “Give the OCR results of the box  $(x_{i,1}^d, y_{i,1}^d, x_{i,2}^d, y_{i,2}^d)$ ”. 3) Line-level OCR. We pick a point near the left side of each line as the position prompt. Then, we construct the line-level multi-turn conversations and an example can be like “OCR the line  $(x_j^d, y_j^d)$ ”. 4) Color-guided OCR. Using the color-text hybrid data in Section 3.2, we define the corresponding cross-vocabulary task by some color-guided questions, such as “OCR red box” and “OCR blue box”. 5) Region-level translation and summary. We filter and retain the boxes with text lengths over 400 on each page. Then, we employ GPT-3.5 [24] to generate the translation and summary for each long in-box text as the corresponding annotations. The instruction can be “Translate/Summarize the content of the box  $(x_{i,1}^d, y_{i,1}^d, x_{i,2}^d, y_{i,2}^d)$ ”. 6) Document layout: We convert the 330K high-quality annotations of PubLayNet [47] to the unified conversation format. Further, we sample 1M extra PDF pages and use PaddleOCRv2 [12] tools to generate pseudo layout annotations.

**In-document figure understanding.** Based on the synthetic interleaved data, we organize the cross-vocabulary image-text pairs into two sub-tasks: 1) In-document figure caption. As a result of the added position-aware prompts, an example language instruction is as follows: “Give a brief description for the region  $(x_1^n, y_1^n, x_2^n, y_2^n)$  of the image”. The box denotes the boundary of the figure. 2) In-document in-figure chat. The RegionChat [46] dataset is built for referential dialogue on natural images. After rendering it on PDF pages, with spatial coordinates of the referring region, we can ask the proposed Fox the following question: “What can you see in this region?  $(x_1^n, y_1^n, x_2^n, y_2^n)$ ”. At a more fine-grained level, the RoI can be the box within the figure on the document page.

**Extension for multi-page documents.** The proposed Fox can be easily tuned to focus on multiple regions of multi-page documents using simple instructions. As a forerunner, we define two basic yet interesting multi-page sub-tasks and give position-aware instruction examples. 1) Multi-page region-level OCR: “OCR boxes on multiple pages. Page 1:  $(x_1^1, y_1^1, x_2^1, y_2^1)$ , Page 2:  $(x_1^2, y_1^2, x_2^2, y_2^2)$ , ... Page N:  $(x_1^N, y_1^N, x_2^N, y_2^N)$ ”. 2) Cross-page VQA: “Which page’s box contains more characters? Page 1:  $(x_1^1, y_1^1, x_2^1, y_2^1)$ , Page 2:  $(x_1^2, y_1^2, x_2^2, y_2^2)$ , ... Page N:  $(x_1^N, y_1^N, x_2^N, y_2^N)$ ”.

It is worth noting that all the above methods are independent of document format. The PDF data with any format or layout, such as single-column, double-column, interleaved, *etc.*, can be parsed to extract positional prompts and formulated into the corresponding conversations. With the fine-grained position-aware instructions, the vision query pipeline enjoys high human-AI interactivity and is robust to different formats (multi-column) and multi-page documents.

### 3.4 Catalyzing Fox by Multi-page and Multi-grained Data Engine

The data engine is a key part of the proposed Fox. To ensure the performance on multiple tasks, We carefully control the quantity and ratio of training data, and more details are reported in Table 1.

**Pre-training data.** In the pre-training stage, we formulate a large number of multimodal task-driven data. Specifically, for hybrid images of in-document caption and chat sub-tasks, we render the BLIP558K [17] data, 1M natural images sampled in Laion-COCO [31] and RegionChat100K [46] data into an equal amount of document pages sampled in prepared PDF data. For fine-grained optical character understanding, we formulate 6 types of 4.6M document image-text pairs, containing box/line/color position-aware prompts and OCR/translation/summary interactive task forms. Further, we generate 800K multi-page data, including multi-page multi-region OCR and cross-page QA. In addition, to maintain the general conversational capabilities of our model, we sample 1M natural data from Laion-COCO [31] and NLP dialogue data from Alpaca [33], Baize [41] and ShareGPT.

**SFT data.** In the supervised fine-tuning stage, To make the conversation experience more comfortable, we sample 10K image-text pairs for each data type of the above pre-training data, and adopt GPT3.5 [24] to rewrite prompts ten times more diversified. Besides, LLaVA80K [17] is also added to further tune our model to generate pleasing answers.

Table 1: Details of multi-page and multi-grained data. In the pre-training phase, we use customized region-level document-text pairs to bring out focusing capabilities.

Task	Region-level Dataset	Sample	Task	Page-level Dataset	Sample
In-document Cap.	PDF×BLIP558K [17]	558K	Layout	PubLayNet [47]	33K
	PDF× Laion-COCO [31]	1M		Annots. by PaddleOCRv2 [12]	1M
In-document Chat	PDF× RegionChat [46]	22K	Cap.	Laion-COCO [31]	500K
Doc. Understanding	foreground OCR	1M	NLP	Alpaca [33]	52K
	region-level OCR	1M		Baize [41]	112K
	line-level OCR	600K		ShareGPT	125K
	color-guided OCR	1M	PDF	Page OCR	1M
	region-level translation	500K		Page Markdown	1M
	region-level summary	500K			
Multi-page Doc.	multi-region OCR	400K	-	-	-
	cross-page VQA	400K	-	-	-

**Input and Conversation Format** For each input image, we resize it with a fixed resolution  $1024 \times 1024$  before feeding it into the SAM-style [14] ViT branch and we perform a resize operation to obtain a new image of  $224 \times 224$  as the input of the CLIP vision network. We choose Qwen-1.8B [2] with rich linguistic vocabulary as our language model. Following the LLaVA-MPT [17, 34] dialogue style, the input conversation format can be summarized as follows: `<lim_start>user: <img>"<image>"</img> "human question [position-aware prompts]"<lim_end><lim_start>assistant: "AI responses" <lim_end>`.

## 4 Experiments

### 4.1 Implementation Details

During the multi-task pre-training and SFT phase, the multiple vision vocabularies (CLIP and SAM-style ViT) are frozen and only the parameters of the embedding linear layers and language model are optimized. We train our model using the optimizer AdamW [20] and a cosine annealing scheduler [19]. The learning rate is set to  $1e-4$  in pretraining and then to  $2e-5$  in SFT. In both stages, we use 48 A800 GPUs with a per device batch of 4 and the data epoch is set to 1.

### 4.2 Multi-grained Benchmark and Metrics

To advance fine-grained document understanding, we build a bilingual benchmark including 9 sub-tasks. We collect 112 English pages and 100 Chinese pages, including single/multi-column formats. The number of words per page exceeds 1,000. These images are used to evaluate page OCR, line-level OCR, color-guided OCR, region-level OCR/translation/summary, multi-page multi-region OCR, and cross-page VQA. Besides, to monitor the performance of interleaved data, we render 200 natural images sampled from Laion-COCO [31] onto 200 PDF pages to evaluate the document-level in-figure caption task. The comprehensive evaluation metrics contain normalized edit distance, F1-score, BLEU [27], METEOR [4], ROUGE [15], and *etc.*

### 4.3 Evaluation Results

**Foreground focus for dense text recognition on a single page.** For the dense text recognition on the entire page, we directly input the normalized box [2, 2, 998, 998] as the foreground prompts. As shown in Table 2 and 3, Fox showcases strong English and Chinese dense OCR ability by almost lossless compression for the document page. Specifically, Fox achieves the best edit distance of 0.046

Table 2: Dense English text recognition on the single document page.

Method	Params	Edit Distance ↓	F1-score ↑	Precision ↑	Recall ↑	BLEU ↑	METEOR ↑
LLaVA-NeXT [16]	34B	0.430	0.647	0.573	0.881	0.478	0.582
InternVL-ChatV1.5 [7]	26B	0.393	0.751	0.698	0.917	0.568	0.663
Nougat [5]	250M	0.255	0.745	0.720	0.809	0.665	0.761
Vary [38]	7B	0.092	0.918	0.906	0.956	0.885	0.926
Vary-toy [39]	1.8B	0.082	0.924	0.919	0.938	0.889	0.929
Qwen-VL-Plus [3]	>100B	0.096	0.931	0.921	0.950	0.893	0.936
Qwen-VL-Max [3]	>100B	0.057	<b>0.964</b>	0.955	<b>0.977</b>	<b>0.942</b>	<b>0.971</b>
Fox (foreground focus)	<b>1.8B</b>	<b>0.046</b>	0.952	<b>0.957</b>	0.948	0.930	0.954

Table 3: Dense Chinese text recognition on the single document page.

Method	Params	Edit Distance ↓	F1-score ↑	Precision ↑	Recall ↑	BLEU ↑	METEOR ↑
InternVL-ChatV1.5 [7]	26B	0.265	0.816	0.784	0.866	0.622	0.717
Vary-toy [39]	1.8B	0.142	0.914	0.928	0.907	0.718	0.832
Qwen-VL-Plus [3]	>100B	0.121	0.895	0.903	0.890	0.684	0.828
Vary [38]	7B	0.113	0.952	0.961	0.944	0.754	0.873
Qwen-VL-Max [3]	>100B	0.091	0.931	0.917	0.946	0.756	0.885
Fox (foreground focus)	<b>1.8B</b>	<b>0.061</b>	<b>0.954</b>	<b>0.964</b>	<b>0.946</b>	<b>0.842</b>	<b>0.908</b>

Table 4: The performance of fine-grained text recognition on the single page. The focusing regions are given by drawn color boxes, coordinates of region boundary, and line points, respectively.

Method	Forms	English			Chinese		
		color	region	line	color	region	line
Fox (region focus)	Edit Distance ↓	0.064	0.059	0.116	0.114	0.042	0.084
	F1-score ↑	0.940	0.957	0.879	0.884	0.955	0.918
	Precision ↑	0.942	0.962	0.879	0.902	0.966	0.931
	Recall ↑	0.942	0.955	0.883	0.873	0.947	0.909
	BLEU ↑	0.868	0.914	0.845	0.778	0.885	0.825
	METEOR ↑	0.938	0.955	0.878	0.848	0.934	0.886

and 0.061 in English and Chinese, respectively. Compared to Vary-toy using the image-level prompts, the proposed Fox lifts the English F1-score by 2.8% by redefining the task as foreground focus. Note that the performance of LLaVA-NeXT and InternVL-ChatV1.5 which use the CLIP-style vocabulary is bottle-necked, indicating that the dense texts of each patch are not completely encoded.

**Region focusing performance of in-document fine-grained tasks.** As shown in Table 4, Fox can yield excellent OCR results on various metrics under several color-guided/region-level/line-level settings, indicating that our model can accurately recognize the content in these randomly sampled RoIs. In Table 5, for the region-level translation, Fox yields an acceptable METEOR of 0.366 due to the smaller language model of 1.8B parameters. In addition, we evaluate our model on the fine-grained summary task and obtain a decent ROUGE-L-F score of 0.282. It is worth mentioning that this kind of usage similar to a reading pen is exactly what users need more.

**Cross-vocabulary focusing tasks on interleaved pages.** The color-guided task requires cross-vocabulary visual knowledge, *i.e.*, CLIP for recognizing colors and Vary-tiny for capturing texts. Table 4 shows that the decent results (0.940 and 0.884 on English and Chinese F1-score) meet our expectations due to the collaboration across multiple vision vocabularies. For the in-document figure caption task, we render natural images onto document pages and ask our model “*What is this in the box < box >?*”, where  $\langle box \rangle$  is the boundary of the natural image that is pasted into the document page. As shown in Table 5, when handling interleaved data, Fox reaches the METEOR of 0.359 and ROUGE-L-F of 0.396 due to the full reaction of activating multiple vocabularies.

**Exploration for focusing on multiple pages.** To verify the focusing capability of Fox on multi-page documents, we report two relevant results in Table 6. For the multi-page OCR task, we ask



Table 5: The performance of in-document fine-grained understanding tasks. The fine-grained translation/summary/caption tasks are targeted at interpreting in-document text/figure regions.

Fine-grained Translation		Fine-grained Summary			Fine-grained Caption	
BLEU	METEOR	ROUGE-L R	ROUGE-L P	ROUGE-L F	METEOR	ROUGE-L F
0.138	0.366	0.261	0.316	0.282	0.359	0.396

Table 6: The performance of fine-grained tasks on the multi-page (8 pages) documents.

Method	Multi-page (8 pages) multi-region OCR				Cross-page (8 pages) VQA
	Edit Distance ↓	F1-score ↑	BLEU ↑	METEOR ↑	Accuracy ↑
Fox (Ours)	0.084	0.946	0.836	0.805	0.827

the model to output the OCR results of 8 boxes on 8 complex pages (in mixed English/Chinese and mixed single/multi-column formats) in a single-turn conversation. Our Fox still performs an amazing F1-score of 0.946 and achieves true focus anywhere by parsing the entire 8-page document simultaneously. For the cross-page visual question-answering task which requires the model to answer which box has the largest number of characters in multiple cross-page boxes, Fox yields a high accuracy of 0.827, demonstrating that it is easier to perform VQA reasoning based on successfully perceiving dense text of multiple pages.

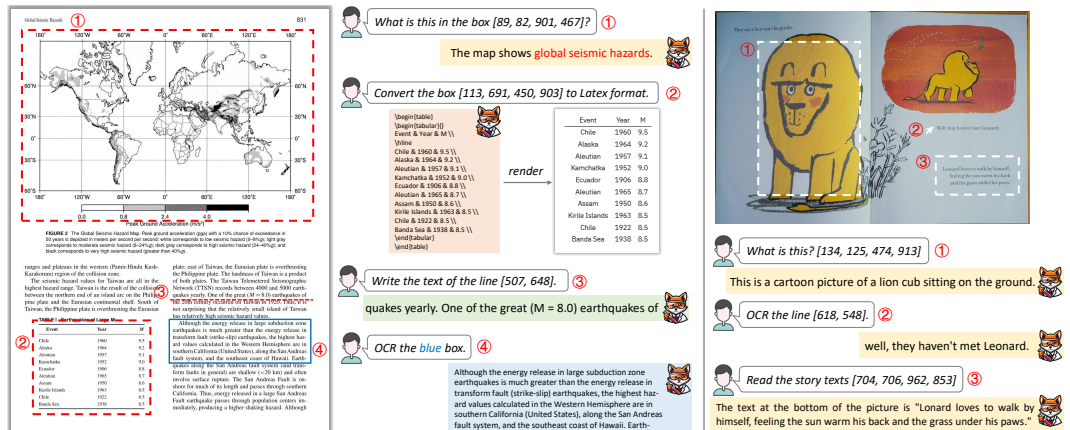


Figure 3: Visualization results. Fox can focus anywhere by supporting fine-grained features, such as in-document figure caption, color-guided OCR, VQA in the cartoon book, and etc.

**Visualization.** Figure 3 shows our Fox can perform impressive features with high human-AI interactivity. For the figure on the academic page, Fox gives the response “global seismic hazards” which is relevant to the content of the document. Fox can also give precise OCR results by dense text perception. For the cartoon book, Fox can recognize the interesting “lion” and can read the story texts for users. This indicates that our Fox enjoys fine-grained focusing capabilities in various scenarios.

## 5 Conclusion and Limitations

This paper proposes a user-friendly LVLM named Fox, which enjoys amazing fine-grained capabilities of focusing anywhere on single/multi-page documents. Further, after catalyzing the multiple vision vocabularies into a full reaction, Fox gains impressive cross-vocabulary features on figure-text interleaved pages. To advance the fine-grained document understanding, we provide a benchmark containing comprehensive sub-tasks. Our Fox can achieve promising scores in these experiments, making a successful step to high human-AI interactivity on dense-content documents. We believe that the proposed method has considerable room for improvement (e.g., the low-resolution CLIP), and we encourage more researchers to focus on more reasonable multi-page document-level tasks.

# 6 Appendix

We show more amazing output results of our model Fox. All testing images are from the Internet.

Writers in Bare Societies

Tribal Political Organization

Writers in Bare Societies

Accumulation of Economic Surplus

The Role of the State

The Role of the State

The Role of the State

The Role of the State

OCR boxes on multiple pages.

Page 1: [110, 417, 898, 641], Page 2: [78, 735, 928, 836],  
Page 3: [510, 190, 928, 483], Page 4: [46, 658, 500, 820],  
Page 5: [500, 502, 896, 742], Page 6: [361, 603, 633, 917],  
Page 7: [518, 336, 950, 528], Page 8: [340, 510, 659, 861].

Whereas bands involve small populations without structure, tribal societies involve at least two well-defined groups linked together in some way and range in population from about 100 to as many as 5,000 people. Though their social institutions can be fairly complex, there are no centralized political structures or offices in the strict sense of those terms. There may be headmen, but there are no rules of succession and sons do not necessarily succeed their fathers as is the case with chiefdoms. Tribal leadership roles are open to anyone—in practice, usually men, especially elder men who acquire leadership positions because of their personal abilities and qualities. Leaders in tribes do not have a means of coercing others or formal powers associated with their positions. Instead, they must persuade others to take actions they feel are needed. A Yanomamí headman, for instance, said that he would never issue an order unless he knew it would be obeyed. The headman Kabawá exercised influence by example and by making suggestions and warning of consequences of taking or not taking an action.<sup>17</sup>

商务礼仪的内容之一是待客之规，包括对商务人员自身的言谈举止、仪表仪容等方面的规范。它也被称为形象设计，要求商务人员严于律己，维护自尊，并且时时守规矩，处处讲规矩、事事有规矩。二是敬人之道，包括商务人员在面对交往对象时进行交际与应酬的基本技巧。具体涉及商务人员从事商务交往的各个方面。

三是突出精品示范园建设，扩大示范带动面。积极建设灵武长枣生态公园，打造“枣乡名城”城市名片；提升建设万亩灵武长枣全国标准化示范园、灵武园艺场无公害、有机化生产示范园，力争每个行政村都有一个精品示范园，以示范园为载体，示范推广应用各类技术，把示范园作为教学基地，紧抓生产管理中的每一个技术环节，广泛开展多种形式的科技培训活动，提高生产者经营者的管理素质水平，开发精品和特色产业，以精品和特色产业为基础，发展生态农业、观光农业、农家乐采摘游和百里枣乡一日游。

b. Each contribution to the custodial account shall identify the depositor's account number and be accompanied by a signed statement directing the investment of that contribution. The Custodian may return to the depositor, without liability for interest thereon, any contribution which is not accompanied by adequate account identification or an appropriate signed statement directing investment of that contribution.

滑行道连接跑道和停机坪，每个跑道可能有几个入口点和出口点。这些点连接着滑行道和跑道。有时候，准备离港的航班在进入跑道前必须等待，这可以在一个（跑道）等待点完成。在等待点，航班也可以被保持或改变沿滑行道顺序，但这是非常罕见的做法。地面控制员负责跑道和停机坪或跑道和停机坪之间的地面运动。他的任务是指导正在滑行的航班在一定的时间内快速、安全的从跑道到达指定停放的位置。反之亦然。时间限制通常来自滑行道的其他部分。停机坪和滑行道有时候地面控制员的任务也包括为机身分配滑行道，但是在许多机场，都有标准的滑行道线。

【牛场村】 向阳镇钱圩行政村，位于向阳镇西北部，东邻姚岭乡，西靠大明行政村，南与太平行政村交界，北接海洲行政村，村委会驻青岗始自然屯，距离镇政府 14 千米，距离县址 56.5 千米，由 17 个村民小组组成，村民分布在其范围内的老架田、再架岭、三义湾、坪上、埃里、船形、新寨、平桃、大亮山、大坝、小亮山、牛场、青岗始、烂料、交老、烂黄、小金岗、金洞、下茶西、外若等 16 个自然屯。1965 年，有耕地面积 3625 亩，全村 375 户 1509 人，有壮、汉、瑶等民族。经济主要以农业为主，主种

At the end of the convention these results were discussed by panelists seated left to right as follows: Noel Lee (Monster), Michael Premer (The Absolute Sound), Ian Eales (a cable believer), Peter Sulheim, Eugene Pitts, Richard Greiner, and Floyd Toole. Clark said this seating order was accidental, but nobody believed him. The two-hour discussion was argumentative, unrevealing, and inconclusive. Audience "questions" were mostly speeches defending pro or anti ideologies. The only agreement that emerged was that people who report hearing cable and amp differences should come part of a controlled testing program to find out what they had to say.

Here, once LIBOR ceases to be published, the trustee of the securitization trust, as the owner of the note, gets to "choose a new index that is based upon comparable information." This is great for the trustee, perhaps not so much for the borrower. Even more, "comparable information" is a vague term that is sure to be the subject of litigation. There are legislative solutions (both adopted and proposed) to the problem of litigation over the trustee's choice of a replacement rate that offer answers to this question. However, uncertainty—and hence substantial litigation risk—remains on the ultimate scope or effectiveness of those legislative solutions.

Figure 4: Fox can give precise responses when focusing on the 8-page document. These pages contain bilingual content, have well over a thousand characters per page, and have a variety of single and multi-column layouts. This extreme case demonstrates powerful focusing capabilities.

Which page's box contains more characters?

① Page 1: [110, 417, 898, 641], ② Page 2: [78, 735, 928, 836],  
 ③ Page 3: [510, 190, 928, 483], ④ Page 4: [46, 658, 500, 820],  
 ⑤ Page 5: [500, 502, 896, 742], ⑥ Page 6: [361, 603, 633, 917],  
 ⑦ Page 7: [518, 336, 950, 528], ⑧ Page 8: [340, 510, 659, 861].

1

Give the OCR results of the box [76, 58, 917, 906].

300

四川广播电视大学学报论丛

另外从环境的角度来看，由于航班滑行燃油消耗效率非常低，导致了机场附近区域很高的排放量。从这些观察中可以看到，设计和优化航班滑行的交通流量的要求提高了，同时还要保持和提高安全的现有水平。

二、优化滑行流程的重要性

(一) 机场地面结构概况

航班降落后才能从跑道进入，因为其他起降的航班还要使用跑道。起飞的航班要从机坪驶向跑道，降落后的航班要驶出跑道停到机坪上。中途经过的阶段是滑行道。换句话说滑行道就是连接跑道与机坪的通道。同时，滑行道也可将性质不同的各功能分区（飞行区、候机楼区、飞行停放区、维修区及供应区）连接起来，使航班最大限度地发挥其容量潜力并提高运行效率。一般的跑道在两端都有出口和滑行道相连，较长的跑道在中段也有出口，以便较短距离不很长的航班能够迅速离开跑道。

航班在滑行道上运动很慢，占用的时间较长。而等待起飞的航班此时满载着燃油重量也最大。所以滑行道除了不必承受飞机降落时的冲击力外，其他方面的载荷比跑道也大小不小。由于这个原因，对滑行道的标准和要求与跑道是相同的。机坪是旅客上下航班、货物装卸的地方，也是航班停放、过夜及维修的场所。机坪可分为停机坪及登机坪两部分。停机坪离候机楼较远，航班在此停放过夜，航班的活动不多。登机坪靠近候机楼，是航班在这里完成它出发的各种准备工作。中途停航的航班要在此处接待上下旅客、装卸货物、添加燃油及接受各种补给和服务工作。为了提高航班的使用率和机场的使用率，以上工作都要抓紧时间进行。过往航班的过站工作通常要求在40分钟内完成。这就使登机坪机坪变得非常繁忙。每一架航班起飞前和降落后至少有十多辆地面车辆围着它提供服务。首先开过来的是自动登机梯，旅客用它来上下航班；运货拖车和可移动式传送带是用来给航班装卸货物的；随车加油车、清洁车、食品供应车、升降平台、电瓶车等纷纷到来，加油车给航班加足燃油；清洁车上的人工把各种卫生用品送上航班，再把机上的垃圾和污水运走；食品供应车给航班上的人提供各种食品和饮料；供水车供应航班上所需的水；升降平台用于维修人员检修飞机外部检查或清理污水时使用。它可以升到10米左右的高度，为维修人员接触航班的各部位。电瓶车是为一些没有辅助动力装置的中小型航班供电。最后到达的是推出拖车，它是专门用于推出航班的，因为航班要靠桥时，机头都是朝向候机楼的，但当航班要离开时，在此无法自行掉头。这时拖车的推出拖车钻到航班下方，挂住航班前轮，把航班推出廊桥区，拖到一定位置，然后它松开接头脱离航班。航班这时才能开始自己滑动。

(二) 滑行过程概述

对于航班来说，滑行过程是它在机场总体周转过程的一部分。一架航班的周转开始于当它被引导穿过空域到达跑道的接近阶段。降落后，航班滑行到它的分配位置或停靠位置。这个停靠位置成为停机坪。这是上下乘客和装卸行李、货物的地方，也是航班为接下来的离港做准备的地方。当航班就绪，并且得到许可，就可以滑行到它将要起飞的目的地离港跑道。

滑行道连接跑道和停机坪。每个跑道可能有几个入口点和出口点。这些点连接着滑行道和跑道。有时候，准备离港的航班在进入跑道并且起飞前必须等待，这可以在一个（跑道）等待点完成。在等待点，航班也可以被保持或改变滑行路径的顺序，但这种不是常见的做法。

地面控制员负责跑道和停机位或跑道和停机坪之间的地面运动。他的任务是指导正在滑行的航班在一定的限制时间内快速、安全的从跑道到达指定停靠的位置。反之亦然，时间限制通常来自周转过程的其他阶段——到港、停靠和离港。有时候地面控制员的任务也包括为机身分配滑行路线。但是在许多机场，都有标准的滑行路线。

滑行过程依赖于周转的其他过程。这个过程将为滑行过程提供时间和位置要求。以下给出了一个简短的关于过程和要求的描述，也显示了如何推动出行时间约束。一架将要到港的航班在它的接近阶段要求从跑道控制员那里得到着陆许可。着陆时间被估算为估计到达时间（ETA），实际到达时间（ATA）指的是飞机到达跑道的实际时间。ETA和ATA由到港管理系统提供。航班着陆后并

Figure 5: The left case shows Fox can handle the cross-page VQA task on the multi-page (8 pages as an example) document. The right case shows Fox can perform the dense Chinese text recognition by foreground focus and obtain precise results.



positives (FP) via center points yet cannot solve the scenario that a center point of the third object lies exactly within the center of an FP. However, this scenario often occurs in some datasets, such as aircraft parked side by side in aerial images. CentripetalNet cannot address the object occlusion problem due to the center overlapping, e.g., pedestrian detection scenario. In summary, existing heuristic corner grouping methods are dataset (COCO [Lin et al., 2014]) driven with poor generalization, but much less effort has been paid to solve it. To tackle this problem, we propose the Corner Affinity, whose motivation is to cover all scenarios aforementioned and bring robust grouping capability for corner-guided detector.

Specifically, Corner Affinity embeds three attributes for each target corner, i.e., locations, shapes, and semantic. Locations and shapes are embedded in the structure affinity (SA) that is a key part of the Corner Affinity, in which we encode the shape (e.g., width and height) knowledge of each instance in its corner location via a strong supervision manner. SA only embedded low-level construction similarity of corners is not enough to accomplish grouping in some extreme scenarios, such as two objects with similar shapes coincide. To this end, we devise the contexts affinity (CA) part for Corner Affinity, in which we utilize the pull-push [Newell et al., 2017; Law and Deng, 2018] algorithm to mine high-level semantic similarity of the corresponding corner pairs to make coincident objects distinguishable. In the CA part, the affinity value is encoded upon the contexts response of instance in a self-supervision manner with no need for a real ground-truth value. Besides, to make the two affinities better interact, we devise the Corner Affinity function, which runs as coupling CA and SA. In this way, SA and CA interplay so that even if the SA value of two corners belong to different instances is large, CA will decay it to make sure that the value of overall Corner Affinity is low, vice versa.

We select three datasets covering different detection scenarios, i.e., COCO [Lin et al., 2014], Citypersons [Cords et al., 2016], and UCAS-AOD [Zhu et al., 2015], to verify the effectiveness of our design. Experimental results show that the proposed Corner Affinity boosts AP of 5.8%, 35.8%, and 17.2%, on the above three benchmarks upon CornerNet baseline, proving the solid effectiveness of our design. We hope the efficient Corner Affinity can attract more attention to promote the development of bionic corner-guided detector.

## 2 Related Work

### 2.1 Center-guided Detector

Center-guided detectors generally use potential center points/areas, acting as reference positives, to regress the object bounding box (e.g., height and width). Classical anchor-based detector belongs in this field, which regards center as an attribute of the preset anchors. Faster R-CNN [Ren et al., 2015] popularizes the center-guided anchor mechanism in its Region Proposal Network (RPN). The aim of RPN is generating a few of proposals from a set of candidate boxes that are encoded via their centers along with heights and widths. In addition, the design of the center-guided RPN makes the detector can be end-to-end trainable. Afterwards, the center-

driven anchor boxes are widely used in RPN-based two-stage detectors. To further explore the efficiency of models, some center-guided one-stage detectors also appeared. They remove the RPN and directly do regression and classification at the centers of anchor boxes. For example, SSD [Liu et al., 2016] improves the performance via densely placing center anchors in multiple layers.

Unlike the center-guided anchor-based detectors [Redmon and Farhadi, 2017; Liu et al., 2016; Lin et al., 2017b], FCOS [Tan et al., 2019] proposes a center-guided anchor-free manner. It treats lots of pixels in center areas of bounding boxes as positive samples and directly regresses four vectors (the distances from each pixel to the corresponding box's borders) without anchor guidance. Instead of four vectors, Repoints [Yang et al., 2019] predicts a set of representative points in the center area (positive pixels).

Despite the center-guided mechanism's great success, it is actually difficult to pinpoint the center of a box. This is because a center requires to be determined via all four boundaries of the object, needing four degrees of freedom.

### 2.2 Corner-guided Detector

Corner-guided detectors usually predict corners via outputting heatmaps, which we argue is more bionic in the generation of the object bounding box. Intuitively, when we want to obtain high-quality bounding boxes manually, each box is labeled from the top-left corner to the bottom-right one and we rarely label the object box by a center point along with height and width. A corner only needs two boundaries (degrees of freedom) to be determined.

CornerNet [Law and Deng, 2018] detects objects by predicting and grouping pairs of corner points. The grouping method in CornerNet is that if a top-left corner and a bottom-right corner belong to the same object, the distance between their embedding vectors will be small. To further optimize this grouping strategy, CenterNet [Duan et al., 2019] adds a prediction branch of center points based on corners pairs estimation, making the corners matching become triplets matching. CentripetalNet [Dong et al., 2020] proposes a new centripetal grouping approach to match paired corner points and achieves state-of-the-art performance.

To sum up, corner grouping is meaningful yet challenge for this kind of detector. Our Corner Affinity aims to produce more robust corner pairs to further advance the development of such human-like corner-guided detector.

## 3 Method

As shown in Figure 2, the execution of Corner Affinity requires an output of the corresponding corner affinity map. Each (top-left or bottom-right) map is composed of three channels, i.e., two for encoding the structure affinity (SA, blue arrow-lines) and one for the contexts affinity (CA, green arrow-lines). The SA and CA interact via a devised function to be the overall Corner Affinity. In the following subsections, we will detail the SA, CA, and Corner Affinity function.

### 3.1 The Structure Affinity

The structure affinity (SA) is a key part of Corner Affinity, aiming to mine preliminary construction similarity of cor-

ners (FP) via center points yet cannot solve the scenario that a center point of the third object lies exactly within the center of an FP. However, this scenario often occurs in some datasets, such as aircraft parked side by side in aerial images. CentripetalNet cannot address the object occlusion problem due to the center overlapping, e.g., pedestrian detection scenario. In summary, existing heuristic corner grouping methods are dataset (COCO [Lin et al., 2014]) driven with poor generalization, but much less effort has been paid to solve it. To tackle this problem, we propose the Corner Affinity, whose motivation is to cover all scenarios aforementioned and bring robust grouping capability for corner-guided detectors.

Specifically, Corner Affinity embeds three attributes for each target corner, i.e., locations, shapes, and semantic. Locations and shapes are embedded in the structure affinity (SA) that is a key part of the Corner Affinity, in which we encode the shape (e.g., width and height) knowledge of each instance in its corner location via a strong supervision manner. SA only embedded low-level construction similarity of corners is not enough to accomplish grouping in some extreme scenarios, such as two objects with similar shapes coincide. To this end, we devise the contexts affinity (CA) part for corner Affinity, in which we utilize the pull-push [Newell et al., 2017; Law and Deng, 2018] algorithm to mine high-level semantic similarity of the corresponding corner pairs to make coincident objects distinguishable. In the CA part, the affinity value is encoded upon the contexts response of instance in a self-supervision manner with no need for a real ground-truth value. Besides, to make the two affinities better interact, we devise the Corner Affinity function, which runs as coupling CA and SA. In this way, SA and CA interplay so that even if the SA value of two corners belong to different instances is large, CA will decay it to make sure that the value of overall Corner Affinity is low, vice versa.

We select three datasets covering different detection scenarios, i.e., COCO [Lin et al., 2014], Citypersons [Cords et al., 2016], and UCAS-AOD [Zhu et al., 2015], to verify the effectiveness of our design. Experimental results show that the proposed Corner Affinity boosts AP of 5.8%, 35.8%, and 17.2%, on the above three benchmarks upon CornerNet baseline, proving the solid effectiveness of our design. We hope the efficient Corner Affinity can attract more attention to promote the development of bionic corner-guided detector.

## Related Work

### 2.1

#### Center-guided Detector

Center-guided detectors generally use potential center points/areas, acting as reference positives, to regress the object bounding box (e.g., height and width). Classical anchor-based detector belongs in this field, which regards center as an attribute of the preset anchors. Faster R-CNN [Ren et al., 2015] popularizes the center-guided anchor mechanism in its Region Proposal Network (RPN). The aim of RPN is generating a few of proposals from a set of candidate boxes that are encoded via their centers along with heights and widths. In addition, the design of the center-guided RPN makes the detector can be end-to-end trainable. Afterwards, the center-driven anchor boxes are widely used in RPN-based two-stage detectors. To further explore the efficiency of models, some center-guided one-stage detectors also appeared. They remove the RPN and directly do regression and classification at the centers of anchor boxes. For example, SSD [Liu et al., 2016] improves the performance via densely placing center anchors in multiple layers.

Unlike the center-guided anchor-based detectors [Redmon and Farhadi, 2017; Liu et al., 2016; Lin et al., 2017b], FCOS [Tan et al., 2019] proposes a center-guided anchor-free manner. It treats lots of pixels in center areas of bounding boxes as positive samples and directly regresses four vectors (the distances from each pixel to the corresponding box's borders) without anchor guidance. Instead of four vectors, Repoints [Yang et al., 2019] predicts a set of representative points in the center area (positive pixels).

Despite the center-guided mechanism's great success, it is actually difficult to pinpoint the center of a box. This is because a center requires to be determined via all four boundaries of the object, needing four degrees of freedom.

### 2.2

#### Corner-guided Detector

Corner-guided detectors usually predict corners via outputting heatmaps, which we argue is more bionic in the generation of the object bounding box. Intuitively, when we want to obtain high-quality bounding boxes manually, each box is labeled from the top-left corner to the bottom-right one and we rarely label the object box by a center point along with height and width. A corner only needs two boundaries (degrees of freedom) to be determined.

CornerNet [Law and Deng, 2018] detects objects by predicting and grouping pairs of corner points. The grouping method in CornerNet is that if a top-left corner and a bottom-right corner belong to the same object, the distance between their embedding vectors will be small. To further optimize this grouping strategy, CenterNet [Duan et al., 2019] adds a prediction branch of center points based on corners pairs estimation, making the corners matching become triplets matching. CentripetalNet [Dong et al., 2020] proposes a new centripetal grouping approach to match paired corner points and achieves state-of-the-art performance.

To sum up, corner grouping is meaningful yet challenge for this kind of detector. Our Corner Affinity aims to produce more robust corner pairs to further advance the development of such human-like corner-guided detector.

## 3

### Method

As shown in Figure 2, the execution of Corner Affinity requires an output of the corresponding corner affinity map. Each (top-left or bottom-right) map is composed of three channels, i.e., two for encoding the structure affinity (SA, blue arrow-lines) and one for the contexts affinity (CA, green arrow-lines). The SA and CA interact via a devised function to be the overall Corner Affinity. In the following subsections, we will detail the SA, CA, and Corner Affinity function.

### 3.1

#### The Structure Affinity

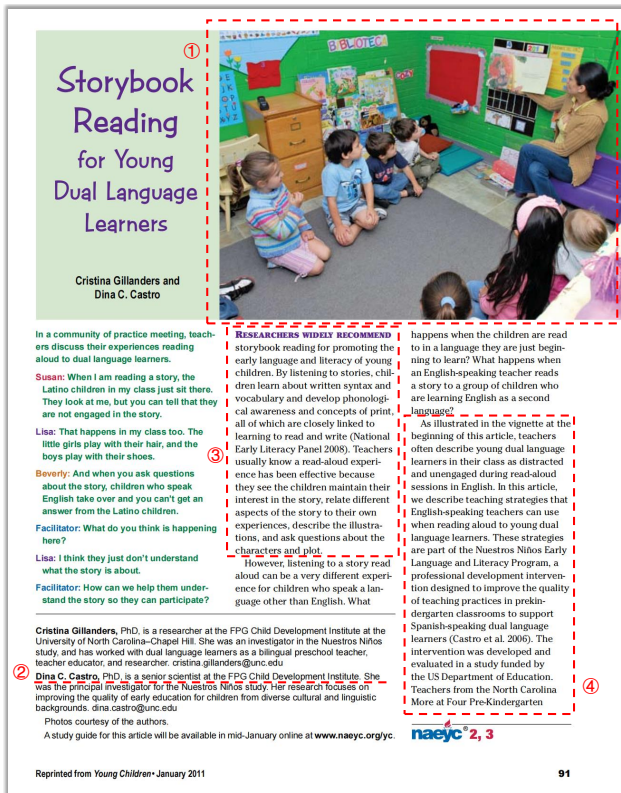
The structure affinity (SA) is a key part of Corner Affinity, aiming to mine preliminary construction similarity of cor-



Give the OCR results of the box [24, 11, 974, 979].

Figure 6: The proposed Fox easily performs dense English text recognition by foreground focus.





**Storybook Reading for Young Dual Language Learners**  
Cristina Gillanders and Dina C. Castro

**Describe the box [354, 41, 992, 405]? ①**  
A woman reading to children about storybooks for **young Dual Language Learners**.

**OCR the line [71, 829]. ②**  
Dina C. Castro, PhD, is a senior scientist at the FPG Child Development Institute. She

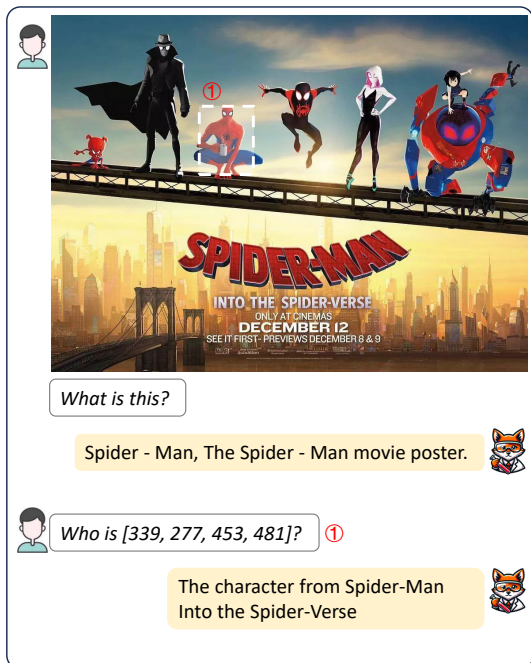
**Translate the area [382, 406, 644, 687]. ③**  
研究员推荐阅读故事书为孩子们提供语言教学。通过倾听故事，孩子们学会像第二语言的孩子一样学习结构句和词汇，并且能够密切与他们交流。学习朗读和写作（国家早期识字面板2008年）。教师通常会朗读，因为人们已经有效地意识到这些是孩子们在故事中保持兴趣的原因，这与他们自己的经历相关。

**Summarize the region [655, 517, 929, 875]. ④**  
Teachers at the Spanish-speaking dual language learners are encouraged to describe their own language learning strategies by sharing with others. This includes reading aloud to young children and using language resources like storybooks and videos. The US Department of Education offers more resources for pre-kindergarten students.

**What is this?**  
Spider - Man, The Spider - Man movie poster.

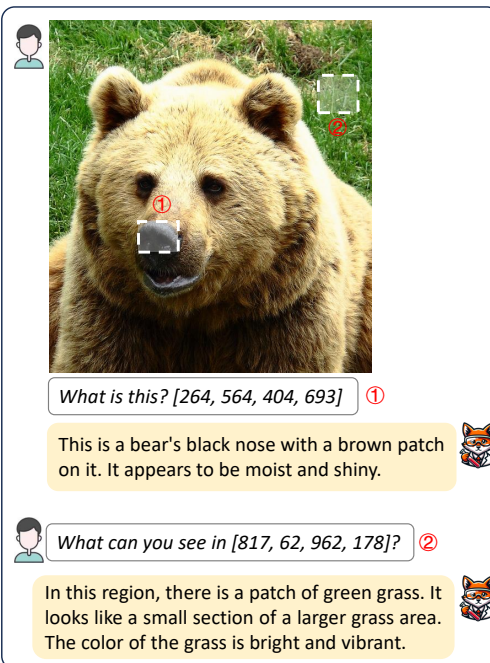
**Who is [339, 277, 453, 481]? ①**  
The character from Spider-Man Into the Spider-Verse

Figure 7: Fox can achieve text-associative in-page figure caption and fine-grained document understanding. Fox enjoys high flexibility and robustness when performing fine-grained region-level translation/summary/OCR tasks in multi-column documents.



**What is this?**  
Spider - Man, The Spider - Man movie poster.

**Who is [339, 277, 453, 481]? ①**  
The character from Spider-Man Into the Spider-Verse



**What is this? [264, 564, 404, 693] ①**  
This is a bear's black nose with a brown patch on it. It appears to be moist and shiny.

**What can you see in [817, 62, 962, 178]? ②**  
In this region, there is a patch of green grass. It looks like a small section of a larger grass area. The color of the grass is bright and vibrant.

Figure 8: Of course, Fox can yield interesting results in cartoon and natural scenes.



## References

- [1] Alayrac, J., Donahue, J., Luc, P., Miech, A., Barr, I., Hasson, Y., Lenc, K., Mensch, A., Millican, K., Reynolds, M., Ring, R., Rutherford, E., Cabi, S., Han, T., Gong, Z., Samangooei, S., Monteiro, M., Menick, J.L., Borgeaud, S., Brock, A., Nematzadeh, A., Sharifzadeh, S., Binkowski, M., Barreira, R., Vinyals, O., Zisserman, A., Simonyan, K.: Flamingo: a visual language model for few-shot learning. In: NeurIPS (2022) [1](#), [3](#)
- [2] Bai, J., Bai, S., Chu, Y., Cui, Z., Dang, K., Deng, X., Fan, Y., Ge, W., Han, Y., Huang, F., Hui, B., Ji, L., Li, M., Lin, J., Lin, R., Liu, D., Liu, G., Lu, C., Lu, K., Ma, J., Men, R., Ren, X., Ren, X., Tan, C., Tan, S., Tu, J., Wang, P., Wang, S., Wang, W., Wu, S., Xu, B., Xu, J., Yang, A., Yang, H., Yang, J., Yang, S., Yao, Y., Yu, B., Yuan, H., Yuan, Z., Zhang, J., Zhang, X., Zhang, Y., Zhang, Z., Zhou, C., Zhou, J., Zhou, X., Zhu, T.: Qwen technical report. arXiv preprint arXiv:2309.16609 (2023) [7](#)
- [3] Bai, J., Bai, S., Yang, S., Wang, S., Tan, S., Wang, P., Lin, J., Zhou, C., Zhou, J.: Qwen-vl: A versatile vision-language model for understanding, localization, text reading, and beyond. arXiv preprint arXiv:2308.12966 (2023) [4](#), [8](#)
- [4] Banerjee, S., Lavie, A.: Meteor: An automatic metric for mt evaluation with improved correlation with human judgments. In: Proceedings of the acl workshop on intrinsic and extrinsic evaluation measures for machine translation and/or summarization. pp. 65–72 (2005) [7](#)
- [5] Blecher, L., Cucurull, G., Scialom, T., Stojnic, R.: Nougat: Neural optical understanding for academic documents. arXiv preprint arXiv:2308.13418 (2023) [8](#)
- [6] Chen, K., Zhang, Z., Zeng, W., Zhang, R., Zhu, F., Zhao, R.: Shikra: Unleashing multimodal llm’s referential dialogic magic. arXiv preprint arXiv:2306.15195 (2023) [2](#)
- [7] Chen, Z., Wang, W., Tian, H., Ye, S., Gao, Z., Cui, E., Tong, W., Hu, K., Luo, J., Ma, Z., et al.: How far are we to gpt-4v? closing the gap to commercial multimodal models with open-source suites. arXiv preprint arXiv:2404.16821 (2024) [1](#), [2](#), [4](#), [8](#)
- [8] Chiang, W.L., Li, Z., Lin, Z., Sheng, Y., Wu, Z., Zhang, H., Zheng, L., Zhuang, S., Zhuang, Y., Gonzalez, J.E., Stoica, I., Xing, E.P.: Vicuna: An open-source chatbot impressing gpt-4 with 90%\* chatgpt quality. <https://lmsys.org/blog/2023-03-30-vicuna/> (2023) [1](#), [3](#)
- [9] Christiano, P.F., Leike, J., Brown, T., Martic, M., Legg, S., Amodei, D.: Deep reinforcement learning from human preferences. Advances in neural information processing systems **30** (2017) [3](#)
- [10] Devlin, J., Chang, M.W., Lee, K., Toutanova, K.: Bert: Pre-training of deep bidirectional transformers for language understanding. arXiv preprint arXiv:1810.04805 (2018) [3](#)
- [11] Dong, L., Yang, N., Wang, W., Wei, F., Liu, X., Wang, Y., Gao, J., Zhou, M., Hon, H.W.: Unified language model pre-training for natural language understanding and generation. Advances in neural information processing systems **32** (2019) [3](#)
- [12] Du, Y., Li, C., Guo, R., Cui, C., Liu, W., Zhou, J., Lu, B., Yang, Y., Liu, Q., Hu, X., et al.: Pp-ocrv2: Bag of tricks for ultra lightweight ocr system. arXiv preprint arXiv:2109.03144 (2021) [6](#), [7](#)
- [13] Ilharco, G., Wortsman, M., Wightman, R., Gordon, C., Carlini, N., Taori, R., Dave, A., Shankar, V., Namkoong, H., Miller, J., Hajishirzi, H., Farhadi, A., Schmidt, L.: Openclip (Jan 2024). <https://doi.org/10.5281/zenodo.10469088>, <https://doi.org/10.5281/zenodo.10469088> [1](#), [4](#)
- [14] Kirillov, A., Mintun, E., Ravi, N., Mao, H., Rolland, C., Gustafson, L., Xiao, T., Whitehead, S., Berg, A.C., Lo, W.Y., et al.: Segment anything. arXiv preprint arXiv:2304.02643 (2023) [1](#), [4](#), [7](#)
- [15] Lin, C.Y.: Rouge: A package for automatic evaluation of summaries. In: Text summarization branches out. pp. 74–81 (2004) [7](#)
- [16] Liu, H., Li, C., Li, Y., Li, B., Zhang, Y., Shen, S., Lee, Y.J.: Llava-next: Improved reasoning, ocr, and world knowledge (January 2024), <https://llava-vl.github.io/blog/2024-01-30-llava-next/> [1](#), [2](#), [4](#), [8](#)
- [17] Liu, H., Li, C., Wu, Q., Lee, Y.J.: Visual instruction tuning (2023) [3](#), [5](#), [6](#), [7](#)
- [18] Liu, Y., Yang, B., Liu, Q., Li, Z., Ma, Z., Zhang, S., Bai, X.: Textmonkey: An ocr-free large multimodal model for understanding document. arXiv preprint arXiv:2403.04473 (2024) [1](#), [2](#), [4](#)
- [19] Loshchilov, I., Hutter, F.: Sgdr: Stochastic gradient descent with warm restarts. arXiv preprint arXiv:1608.03983 (2016) [7](#)

- [20] Loshchilov, I., Hutter, F.: Decoupled weight decay regularization. In: ICLR (2019) 7
- [21] Lu, H., Liu, W., Zhang, B., Wang, B., Dong, K., Liu, B., Sun, J., Ren, T., Li, Z., Sun, Y., et al.: Deepseek-vl: towards real-world vision-language understanding. arXiv preprint arXiv:2403.05525 (2024) 3
- [22] Mishra, A., Shekhar, S., Singh, A.K., Chakraborty, A.: Ocr-vqa: Visual question answering by reading text in images. In: 2019 international conference on document analysis and recognition (ICDAR). pp. 947–952. IEEE (2019) 1
- [23] Moysset, B., Kermorvant, C., Wolf, C.: Full-page text recognition: Learning where to start and when to stop. In: 2017 14th IAPR International Conference on Document Analysis and Recognition (ICDAR). vol. 1, pp. 871–876. IEEE (2017) 3
- [24] OpenAI: Chatgpt. <https://openai.com/blog/chatgpt/> (2023) 3, 6, 7
- [25] OpenAI: Gpt-4 technical report (2023) 1
- [26] Ouyang, L., Wu, J., Jiang, X., Almeida, D., Wainwright, C.L., Mishkin, P., Zhang, C., Agarwal, S., Slama, K., Ray, A., Schulman, J., Hilton, J., Kelton, F., Miller, L., Simens, M., Askell, A., Welinder, P., Christiano, P.F., Leike, J., Lowe, R.: Training language models to follow instructions with human feedback. In: NeurIPS (2022) 3
- [27] Papineni, K., Roukos, S., Ward, T., Zhu, W.J.: Bleu: a method for automatic evaluation of machine translation. In: Proceedings of the 40th annual meeting of the Association for Computational Linguistics. pp. 311–318 (2002) 7
- [28] Radford, A., Kim, J.W., Hallacy, C., Ramesh, A., Goh, G., Agarwal, S., Sastry, G., Askell, A., Mishkin, P., Clark, J., et al.: Learning transferable visual models from natural language supervision. In: International conference on machine learning. pp. 8748–8763. PMLR (2021) 2, 3, 4, 5
- [29] Radford, A., Wu, J., Child, R., Luan, D., Amodei, D., Sutskever, I., et al.: Language models are unsupervised multitask learners. OpenAI blog 1(8), 9 (2019) 3
- [30] Raffel, C., Shazeer, N., Roberts, A., Lee, K., Narang, S., Matena, M., Zhou, Y., Li, W., Liu, P.J.: Exploring the limits of transfer learning with a unified text-to-text transformer. The Journal of Machine Learning Research 21(1), 5485–5551 (2020) 1, 3
- [31] Schuhmann, C., Vencu, R., Beaumont, R., Kaczmarczyk, R., Mullis, C., Katta, A., Coombes, T., Jitsev, J., Komatsuzaki, A.: Laion-400m: Open dataset of clip-filtered 400 million image-text pairs. arXiv preprint arXiv:2111.02114 (2021) 2, 5, 6, 7
- [32] Smith, R.: An overview of the tesseract ocr engine. In: Ninth international conference on document analysis and recognition (ICDAR 2007). vol. 2, pp. 629–633. IEEE (2007) 3
- [33] Taori, R., Gulrajani, I., Zhang, T., Dubois, Y., Li, X., Guestrin, C., Liang, P., Hashimoto, T.B.: Stanford alpaca: An instruction-following llama model. [https://github.com/tatsu-lab/stanford\\_alpaca](https://github.com/tatsu-lab/stanford_alpaca) (2023) 3, 6, 7
- [34] Team, M., et al.: Introducing mpt-7b: A new standard for open-source, commercially usable llms (2023) 7
- [35] Touvron, H., Lavril, T., Izacard, G., Martinet, X., Lachaux, M.A., Lacroix, T., Rozière, B., Goyal, N., Hambro, E., Azhar, F., Rodriguez, A., Joulin, A., Grave, E., Lample, G.: Llama: Open and efficient foundation language models. arXiv preprint arXiv:2302.13971 (2023) 3
- [36] Vaswani, A., Shazeer, N., Parmar, N., Uszkoreit, J., Jones, L., Gomez, A.N., Kaiser, Ł., Polosukhin, I.: Attention is all you need. Advances in neural information processing systems 30 (2017) 3
- [37] Veit, A., Matera, T., Neumann, L., Matas, J., Belongie, S.: Coco-text: Dataset and benchmark for text detection and recognition in natural images. arXiv preprint arXiv:1601.07140 (2016) 1
- [38] Wei, H., Kong, L., Chen, J., Zhao, L., Ge, Z., Yang, J., Sun, J., Han, C., Zhang, X.: Vary: Scaling up the vision vocabulary for large vision-language models. arXiv preprint arXiv:2312.06109 (2023) 1, 2, 4, 5, 8
- [39] Wei, H., Kong, L., Chen, J., Zhao, L., Ge, Z., Yu, E., Sun, J., Han, C., Zhang, X.: Small language model meets with reinforced vision vocabulary. arXiv preprint arXiv:2401.12503 (2024) 8
- [40] Wei, J., Tay, Y., Bommasani, R., Raffel, C., Zoph, B., Borgeaud, S., Yogatama, D., Bosma, M., Zhou, D., Metzler, D., et al.: Emergent abilities of large language models. arXiv preprint arXiv:2206.07682 (2022) 3

- [41] Xu, C., Guo, D., Duan, N., McAuley, J.: Baize: An open-source chat model with parameter-efficient tuning on self-chat data. arXiv preprint arXiv:2304.01196 (2023) [6](#), [7](#)
- [42] Ye, J., Hu, A., Xu, H., Ye, Q., Yan, M., Xu, G., Li, C., Tian, J., Qian, Q., Zhang, J., et al.: Ureader: Universal ocr-free visually-situated language understanding with multimodal large language model. arXiv preprint arXiv:2310.05126 (2023) [1](#), [2](#), [3](#), [4](#)
- [43] Ye, Q., Xu, H., Xu, G., Ye, J., Yan, M., Zhou, Y., Wang, J., Hu, A., Shi, P., Shi, Y., et al.: mplug-owl: Modularization empowers large language models with multimodality. arXiv preprint arXiv:2304.14178 (2023) [4](#)
- [44] Zeng, A., Liu, X., Du, Z., Wang, Z., Lai, H., Ding, M., Yang, Z., Xu, Y., Zheng, W., Xia, X., et al.: Glm-130b: An open bilingual pre-trained model. arXiv preprint arXiv:2210.02414 (2022) [3](#)
- [45] Zhang, S., Roller, S., Goyal, N., Artetxe, M., Chen, M., Chen, S., Dewan, C., Diab, M., Li, X., Lin, X.V., et al.: Opt: Open pre-trained transformer language models. arXiv preprint arXiv:2205.01068 (2022) [1](#), [3](#)
- [46] Zhao, L., Yu, E., Ge, Z., Yang, J., Wei, H., Zhou, H., Sun, J., Peng, Y., Dong, R., Han, C., et al.: Chatspot: Bootstrapping multimodal llms via precise referring instruction tuning. arXiv preprint arXiv:2307.09474 (2023) [2](#), [5](#), [6](#), [7](#)
- [47] Zhong, X., Tang, J., Yepes, A.J.: Publaynet: largest dataset ever for document layout analysis. In: 2019 International conference on document analysis and recognition (ICDAR). pp. 1015–1022. IEEE (2019) [3](#), [6](#), [7](#)
- [48] Zhu, D., Chen, J., Shen, X., Li, X., Elhoseiny, M.: Minigt-4: Enhancing vision-language understanding with advanced large language models. arXiv preprint arXiv:2304.10592 (2023) [1](#)